

S. L. Crick · F. C.-P. Yin

## Assessing micromechanical properties of cells with atomic force microscopy: importance of the contact point

Received: 1 March 2005 / Accepted: 1 May 2006 / Published online: 15 June 2006  
© Springer-Verlag 2006

**Abstract** Mechanical properties are obtainable from atomic force microscopy (AFM) indentation force–depth curves, which are calculated from relationships between tip deflection and cantilever position, i.e. deflection curves. Indentation depth is the difference between tip deflections on a rigid and a soft material for the same amount of cantilever advancement, after contact is made. Since the contact point cannot be unequivocally identified from experimental data, there is some uncertainty in estimating material properties. Using simulations, this study examines some important issues related to the influence of contact point identification on estimated material properties. Simulations for linear materials using a typical stiffness for an AFM cantilever demonstrate that certain portions of the post-contact region of deflection curves for soft and very stiff materials can be approximated by quadratic and linear functions, respectively. Based on these findings, we first develop and verify an objective, automatic method to identify the contact point for materials with linear properties. We then assess the effect of misidentifying the contact point, with and without noise. If the contact point is missed by  $< 50$  nm, material properties for small indentations are erroneous but the error decreases asymptotically beyond 200 nm of indentation and the correct estimate of material stiffness is obtained. If the contact point is missed by  $> 100$  nm, however, the true material properties cannot be estimated accurately. Noise adds to uncertainty in material properties at small indentations but the combined effect of missing the contact point and noise is dominated by the former. Even though the algorithm was developed for linear materials, it is also suitable for certain nonlinear materials making it more generally applicable.

### 1 Introduction

An atomic force microscope (AFM) can be used as an indenter to probe the nanomechanical properties of small regions of materials — including living cells (Lal and John 1994; Hofmann et al. 1997; Wu et al. 1998; Sato et al. 2000; Tao et al. 1992; Burnham and Colton 1989; Bowen et al. 2000; Heinz and Hoh 1998, 1999; Radmacher 1997; Mathur et al. 2001; Shroff et al. 1995). AFM indentation is simple to apply, but analyzing and correctly interpreting the results is fraught with pitfalls. This is because the mechanical properties of the material being examined can only be obtained indirectly from the indentation force–depth relationship, which, in turn, has to be inferred from the relationship between the deflection of the tip and the vertical position of the cantilever as it is moved toward and then touches the specimen. This latter relationship is usually called a *deflection curve*. The indentation depth, at a given cantilever position after contact with a material, is the difference between the tip deflection on a rigid and the soft material. Indentation depth, and hence the estimated mechanical property, is therefore dependent on the identification of the contact point.

The importance of identifying the contact point is well known but has not been subjected to careful study. For a rigid material, the contact point is rather easily discerned as it demarcates the transition from the approach of the cantilever where there is no deflection to a line with a slope of about unity (since for a given amount of cantilever advance, the tip deflects the same amount). For a material that can be indented, however, the contact point can never be identified with certainty, but rather must be inferred from the deflection curve. Several factors make this identification difficult. First, unless the cantilever tip is flat, once contact has occurred, the relationship between cantilever position and tip deflection is no longer linear. Second, after contact, the tip deflection is not a perfect quadratic function of cantilever position but rather a complicated nonlinear function that depends upon the relative stiffnesses of the cantilever and material. The softer the material and/or the stiffer the cantilever the less tip deflection there

S. L. Crick · F. C.-P. Yin (✉)  
Department of Biomedical Engineering,  
Washington University, Campus Box 1097,  
One Brookings Drive, St. Louis, MO 63130, USA  
E-mail: yin@biomed.wustl.edu  
Tel.: +1-314-9356164  
Fax: +1-314-9357448

will be. This complicated nonlinear effect precludes using a simple function to fit the post-contact portion of all displacement curves. The two factors are exacerbated by the inherent electrical and mechanically-induced noise in the cantilever deflection signal. After initial contact is made, as tip deflection increases with increasing indentation, the signal is easier to discern from the noise. Hence, the initial small indentations, including the contact point, are the most difficult to clearly identify. In fact, this difficulty in identifying the contact point led to an analysis method that attempted to circumvent this problem (A-Hassan et al. 1998). This method provides, however, only relative comparisons between different samples and does not specifically quantify properties of a given material. Therefore, before indentation with AFM can be used reliably to investigate the mechanical properties of a sample, the interrelated effects of misidentifying the contact point and noise in the signal must be elucidated.

Even assuming one has accurately identified the contact point and obtained a force–depth relationship, analytical difficulties remain. For example, the pyramidal or conical geometry of most AFM tips results in an inherently nonlinear force–depth relationship. (Briscoe et al. 1994; Dimitriadis et al. 2002) This tip effect dominates the force–depth relationship, and may obscure subtle differences from the quadratic behavior that characterizes materials with linear stress–strain properties. Several studies indicate that not correctly accounting for tip geometry and hence the resulting mechanics can result in erroneous estimates of material properties, whereas correctly accounting for tip geometry and employing proper mechanical principles, may even enable one to discriminate between different types of materials. (Briscoe et al. 1994; Dimitriadis et al. 2002; Costa and Yin 1999) Additionally, the cantilever deflection must be converted into force using an appropriate calibration scheme. Calibration of AFM cantilevers has also been the subject of many reports, but no clear, widely-accepted method has resulted (Cleveland et al. 1993; D’Costa and Hoh 2005; Hutter and Bechhoefer 1993; Jensen 1993; Scholl et al. 1994; Smith and Howard 1994; Sader et al. 1995; Cumpson et al. 2003; Gibson et al. 2003). For all of the above reasons, the absolute values of the reported mechanical properties are, to some extent, uncertain. Although the issues of tip geometry and calibration are important to accurately assess mechanical properties of cells, addressing them is beyond the scope of the present study. Rather, we focus on issues related to identification of the contact point and how this affects the subsequent determination of the mechanical properties.

The purpose of this study is to carefully examine the above issues. We use simulated data for materials with linear stress–strain relationships covering a wide range of stiffnesses and for some types of materials with nonlinear stress–strain relationships to develop guidelines and an algorithm to semi-automatically identify the contact point. We also use experimental data for an endothelial cell to illustrate the approach. Based on detailed analysis of the post-contact region of simulated deflection curves for the linear materials we propose an objective method to automatically identify the

contact point. This method presumes that the contact point is the transition from the linear to the nonlinear region of the deflection curves. The algorithm not only can identify accurately the contact point for linear materials but it also can do so for some nonlinear materials. We next assess the effect on the mechanical property estimations of misidentifying the contact point, with and without simulated noise, for both linear and nonlinear materials. For linear materials if the contact point is misidentified by 50 nm, there are large errors in the estimated apparent point-by-point modulus ( $E_{pp}$ , Costa and Yin 1999) for indentations less than 200 nm. At indentations greater than 200 nm, however, the value asymptotically approaches the correct value. If the contact point is misidentified by  $\sim 100$  nm or more, however,  $E_{pp}$  cannot be accurately estimated. As expected, the effect of noise is also manifested as uncertainties in material properties at small indentations. Surprisingly, however, for indentations larger than 200 nm the combined effect of misidentifying the contact point and noise is dominated by the former. For nonlinear materials with polynomial stress–strain relationships the effects of misidentifying the contact points are generally similar to those for linear materials. Specifically, misidentifying the contact point by up to five data points produces a nonlinear dependence of  $E_{pp}$  on indentation depth. The error in  $E_{pp}$  is bounded to less than a factor of two at low indentation depths and decreases with increasing indentation depth. For materials with exponential type stress–strain laws, however, opposite results are observed. The same amount of misidentification results in errors of less than a factor of two at indentation depths less than 200 nm. However, the error bounds increase with increasing indentation depth reaching more than an order of magnitude at indentation depths greater than about 400 nm. The highly nonlinear deflection curves of materials with exponential stress–strain behavior appear to render accurate analysis of force-indentation data problematic for this type of material.

The results of this study should serve as a foundation for future studies of AFM indentation in soft materials, including biological tissues and cells.

## 2 Methods

### 2.1 Deflection curves

To address the issues of interest requires some deflection curves for which we know the precise contact point. We convert known force–depth relationships into simulated deflection curves. Note that for any tip that is not flat, the conversion of a force–depth relationship into a deflection curve is not simple because the complex tip geometry must be taken into account. Specifically, even for a perfect cone with a quadratic relationship between indentation force and depth, the tip deflection after contact is not a simple quadratic function of cantilever position. For more complicated, but also more realistic tip geometries, the displacement curve can only be obtained by numerical simulation. In addition to

the effects of tip geometry, the type of material also affects the displacement curve. For a given cantilever stiffness, two factors affect the shape of a deflection curve: material type (i.e. linear vs. nonlinear stress–strain behavior) and the specific values of the material parameters. For materials with linear stress–strain behavior we first calculated the force exerted by a blunt-tip conical indenter on an elastic half-space (Fig. 1), as a function of indentation depth and then converted these force–depth data into deflection curves. To develop the algorithm and assess the effect of different stiffnesses, we compared a range of values of elastic moduli (0.1, 1, 10, 50 and 100 kPa). This wide range of stiffnesses should encompass most biological materials, including cells and their constituents which are thought to be in the 10–50 kPa range.

The simulation first requires the relationship between indentation force and depth and can be expressed in terms of  $E_{pp}$  as previously described (Costa and Yin 1999). The following two-part equation (adopted from Briscoe et al. 1994) is used for calculating the point-by-point modulus for an indenter with the cantilever tip approximated as a cone merging smoothly with a spherical tip (see Fig. 1).

$$1) E_{pp} = \left( \frac{3F(1-\nu^2)}{4h^{\frac{3}{2}}\sqrt{R}} \right) \quad a < b$$

$$2) E_{pp} = \frac{F(1-\nu^2)}{2\Psi} \quad a > b$$

where

$F \equiv$  Indentation Force

$$\Psi = ah - \frac{a^2}{2 \tan(\theta)} \left( \frac{\pi}{2} - \arcsin\left(\frac{b}{a}\right) \right) - \frac{a^3}{3R} + \sqrt{a^2 - b^2} \left( \frac{b}{2 \tan(\theta)} + \frac{a^2 - b^2}{3R} \right)$$

and contact radius  $a(h)$  is calculated from

$$3) h + \frac{a}{R} (\sqrt{a^2 - b^2}) - a - \frac{a}{\tan(\theta)} \left[ \frac{\pi}{2} - \arcsin\left(\frac{b}{a}\right) \right] = 0$$

In this formulation  $b = R \cos(\theta)$  enforces the smoothness constraint and rather than subsuming the Poisson's ratio  $\nu$  into a modified modulus (as suggested by Briscoe et al. 1994; Costa et al. 2006), we use the value of 0.5 which is that for an incompressible, linear, elastic and isotropic material.

The simulated deflection curves for materials with linear stress–strain laws were obtained using an equation solver that allowed simultaneously changing the deflection and contact radius  $a$  (see Fig. 1) subject to the constraints that, when indentation was greater than the height of the spherical tip, the elastic modulus remained constant and that the derivative of the overall force on the tip as a function of contact radius was zero. This latter constraint leads to Eq. 3. When the indentation depth was less than the height of the spherical tip, the only constraint was that the elastic modulus was constant.

The cantilever stiffness used in the simulations was 0.0186 N/m. This value is at the softer end of the stiffness spectrum of the Park, Inc. gold-coated, silicon-nitride cantilevers, but is representative of the values used in our studies on cells. The simulated deflection curves for the different

values of the elastic moduli are shown in Fig. 2a. Even for a linear material, the shape of the deflection curve varies, depending upon the stiffness of the material relative to the stiffness of the cantilever.

For materials with nonlinear stress–strain laws, i.e. nearly linear Mooney–Rivlin (MR), polynomial (POLY) or exponential (EXP) types, we used the force–depth curves previously obtained with a finite-element model of indentation (Costa and Yin 1999). The parameter values chosen for these materials were not necessarily meant to represent any specific material, but rather to give a range of stress–strain behavior from nearly linear to highly nonlinear. The deflection curves from those force–depth curves were obtained by essentially the same procedure as for the linear materials described above and are shown in Fig. 2b.

The simulations indicate that the post-contact deflection curves for all soft materials are nonlinear. The degree of nonlinearity is dependent upon both the stiffness of the linear materials and the specific type of nonlinear material. Restricting attention to linear materials, to see if a single function could adequately describe post-contact deflection curves for this range of stiffnesses, we fit varying percentages of the data with a three-term polynomial (constant, a linear term and a higher order term) letting the exponent of the higher order term be a free parameter. The results are shown in Fig. 3. Though there is no single function that fits all deflection curves, a quadratic function fits well for stiffnesses less than 10 kPa – if more than 30% of the post-contact data are used. For intermediate stiffness, i.e. 10 kPa, a quadratic fit is also reasonable but only if 30% of the initial post-contact data are used. For stiffnesses of 100 kPa or more, a linear fit is a reasonable approximation – but only if more than 75% of the data are used for fitting.

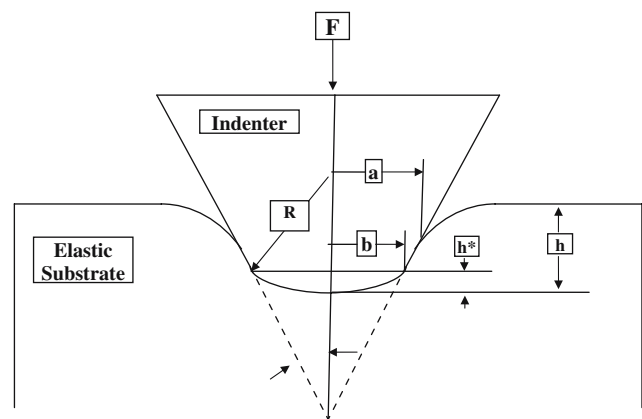


**Fig. 1** Schematic of a cone with a spherical tip indenting an elastic half-space (redrawn from Briscoe et al. 1994) with the following parameters:  $a$  = radius of contact between material and axisymmetric indenter;  $b$  = radius of beginning of cone  $R$  = radius of curvature of spherical tip  $h$  = indentation depth  $h^*$  = height of spherical tip  $\theta$  = semi-included angle of equivalent cone

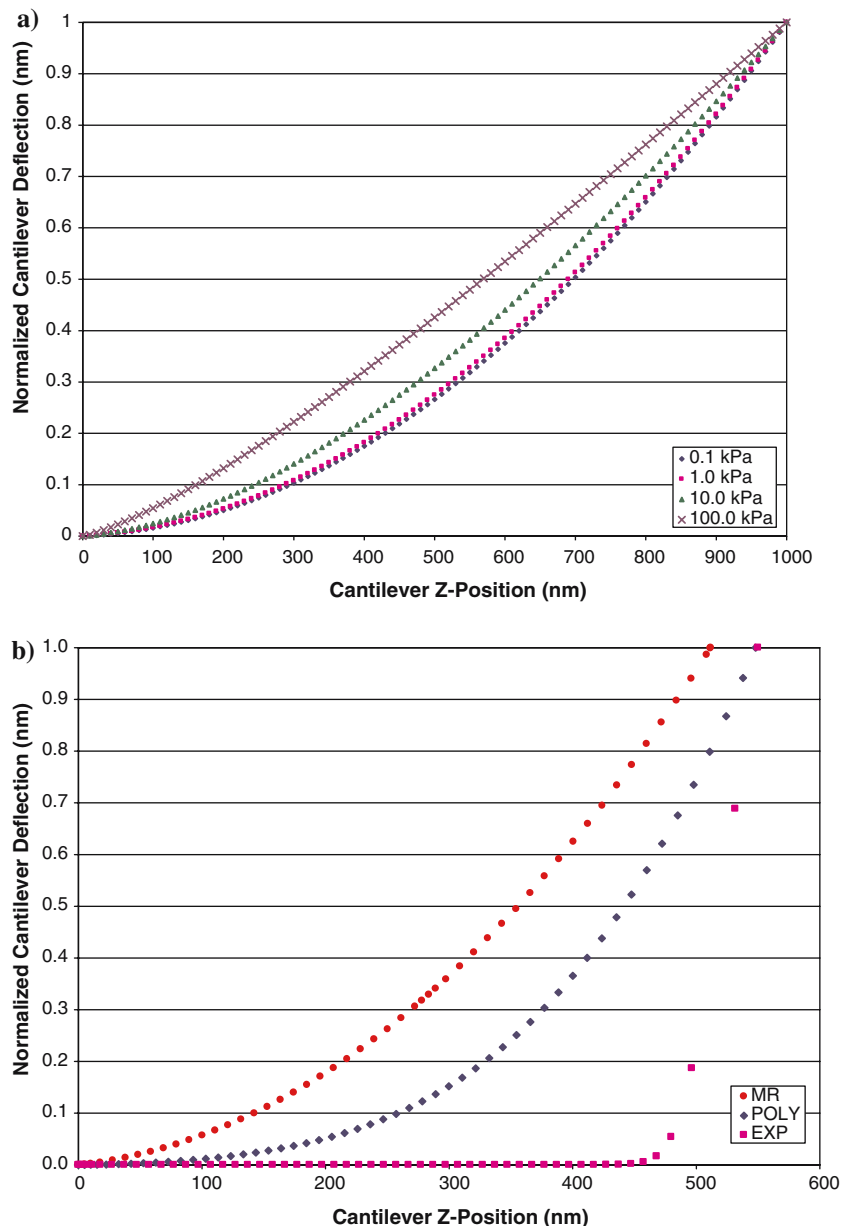


**Fig. 2** **a** Normalized, simulated deflection curves for linear materials of different elastic moduli. All curves were normalized such that the maximum deflection was equal to one. **b** Normalized, simulated deflection curves for materials with Mooney–Rivlin, polynomial and exponential stress–strain laws. All curves have the same contact point located where the cantilever  $z$ -position equals

## 2.2 Identifying the contact point

Based on the above findings, we propose a method to automatically and objectively determine the contact point from deflection curves by assuming that: (1) prior to contact with the sample, the relationship between cantilever position and deflection is linear (with slope close to zero) and changes either to an approximately quadratic one after contact – if the material is not too stiff – or to a linear relationship (with slope much greater than zero) for stiffnesses of 100 kPa and greater. (2) The contact point is the transition between the initial linear and the subsequent quadratic or linear relationships.

The flow chart in Fig. 4 outlines the major features of this algorithm – each of which is summarized below:

- One first needs to determine the noise level of the data. A reasonable assumption is that the fluctuations in the deflection signal prior to contact are due to noise, which can be quantified by the standard deviation of the signal where contact has clearly not occurred. The algorithm is not sensitive to the specific amount of data encompassed – as long as one is certain to include only data where contact has not occurred. A representative deflection curve obtained on an endothelial cell is shown in Fig. 5. While any of a number

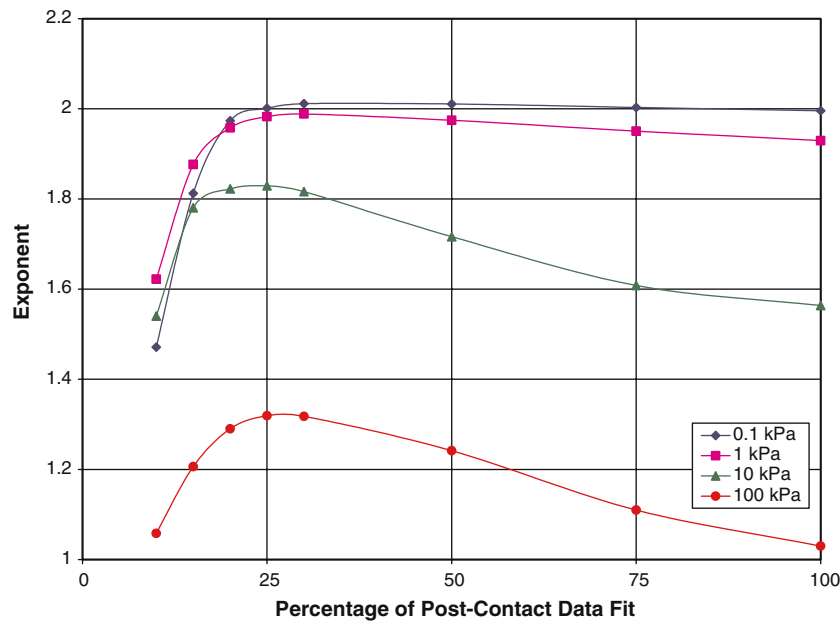


**Fig. 3** Exponents of the best-fit polynomial for the post-contact region for linear materials with different elastic moduli as a function of the amount of data used in the fitting. The simulated deflection versus  $z$ -position curves from which these results were obtained are those shown in Fig. 2

of different approaches can be used to ascertain the noise level, we have found the following empirical scheme to be workable. To avoid possible initial artifacts that can sometimes occur during an experiment, to ensure sufficient data for robust statistics, and to enable automatic quantification of a number of deflection curves, we calculate the standard deviation of the signal in the initial 12.5 to 37.5% of the data (box A in Fig. 5a).

- After contact, as the cantilever is advanced, the tip deflection becomes progressively greater than the noise. Hence, the contact point must be between a lower and an upper bound of the cantilever position. We use the following procedure to find these initial bounds. Beginning with the data used to define the noise level, we examine moving subsets containing 25% of all of the data. When the difference in cantilever deflection between the beginning and the end of the subset is more than eight times the noise level, we presume that contact has occurred. We define the beginning and end of this data subset as the initial lower and upper bound, respectively. Box B in Fig. 5a demonstrates one of these data subsets defining the lower and upper bound.
- The data within the bounds likely contain the contact point. To identify it, we need to make two different fits to the data – one using data before and one after the contact point (see below). As indicated in Fig. 3, depending upon the stiffness, differing amounts of data should be used for fitting. Hence, if the putative contact point is too close to either bound there may be insufficient data to obtain reasonable fits. For example, the contact point for a very stiff material may be very close to the upper bound and vice versa for a very soft material. Hence, the bounds may need some adjusting, depending upon an estimate of the stiffness, to provide sufficient data for an accurate fit. Since

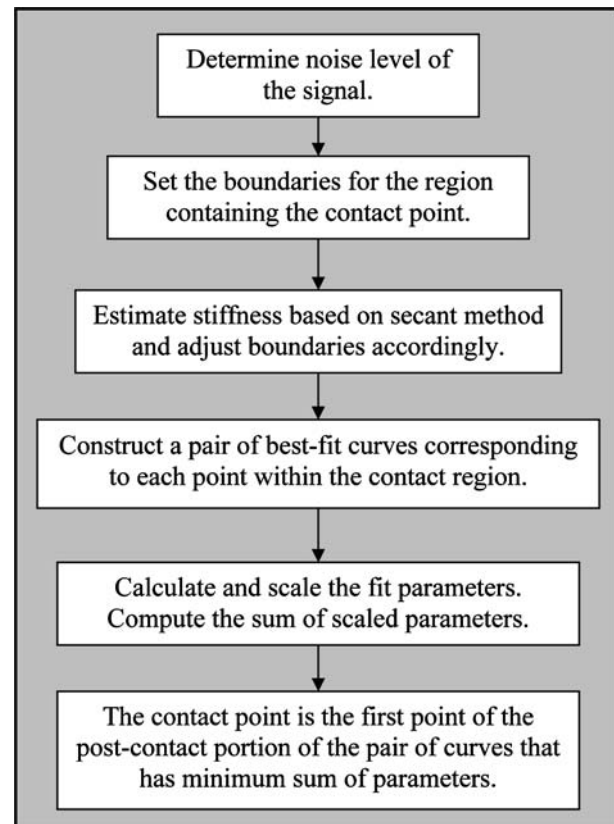
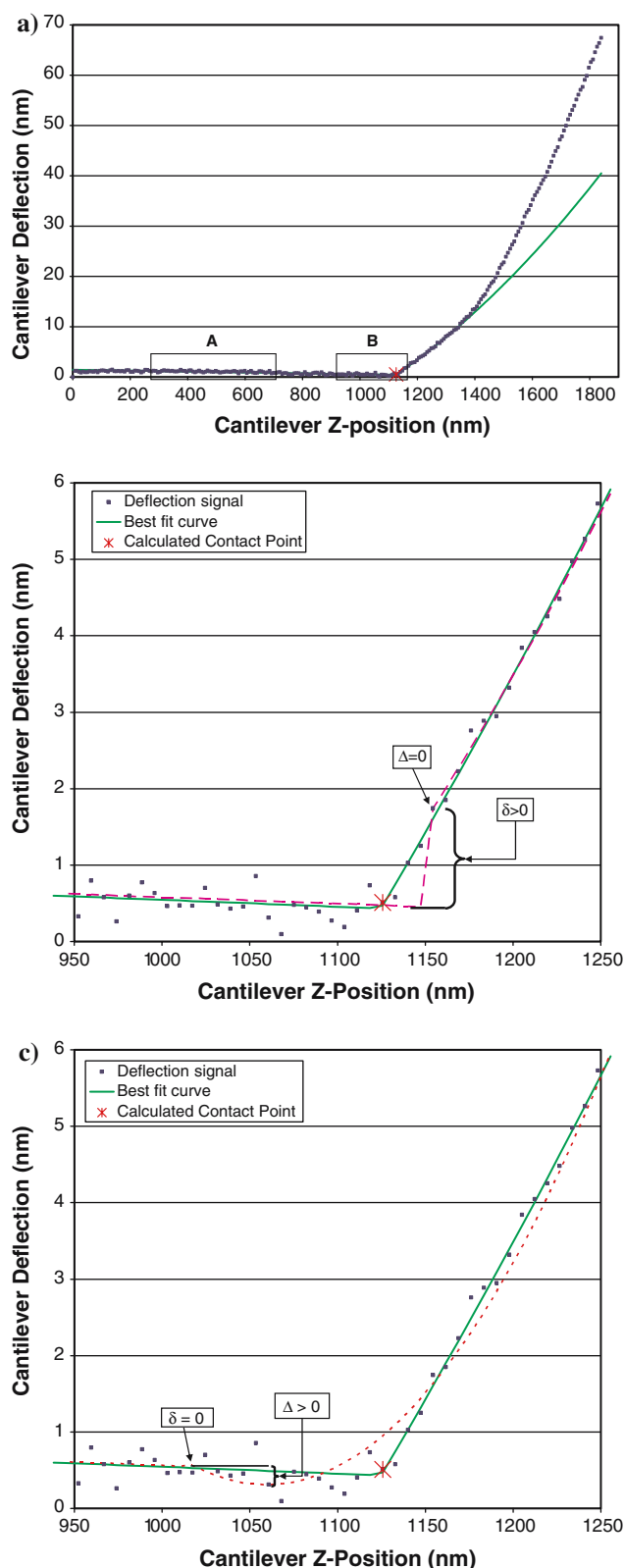


**Fig. 4** Flowchart of the contact point identification algorithm

we only need to distinguish very stiff materials i.e. those of  $> 100$  kPa from softer ones, a crude estimate of stiffness should suffice. Such an estimate can be obtained from the





slope of the secant ( $\Delta y / \Delta x$ ) of the post-contact data, from the initial upper bound to the maximum deflection, as illustrated in Fig. 6a. As shown in the inset to Fig. 6a, the slope

**Fig. 5** a A typical deflection curve for a human aortic endothelial cell. *Box A* denotes the region used to ascertain the noise level of the signal. *Box B* denotes the bounds (the region most likely to contain the actual contact point). The *solid curve* corresponds to the pair of best-fit curves that determines the contact point. Note that the curve only fits well 30% of the post-contact data well. Data were obtained with a Digital Instruments Bioscope operated in a  $4 \times 4$  force-volume mode covering  $5.24 \times 5.24 \mu\text{m}$  at a frequency of 1 Hz with a  $z$ -piezo travel of 2000 nm. The cantilever was from Park Instruments, Inc. and was V-shaped with a length of  $220 \mu\text{m}$  with a stiffness of  $0.0197 \text{ nN/nm}$  as estimated from its natural frequency in air. b An expanded view of the region containing the contact point and best-fit curves (*solid line* and *curve*) of the data shown in (a). The *asterisk* denotes the calculated contact point. The high level of noise is clearly evident in this region. The *dashed line* and *curve* illustrate how the parameters  $\Delta$  and  $\delta$  are defined. The discontinuity,  $\delta$ , is the difference between the end of the linear fit and the beginning of the quadratic fit.  $\Delta$  is the difference between the nadir and the beginning of the quadratic portion. In this example, there is large discontinuity,  $\delta$ , but  $\Delta$  is zero. The *dashed curve* better fits the post-contact data in an RMS sense than the post-contact curve of the best-fit pair, but clearly this curve does not correspond to the contact point. c The same data and nomenclature as (b) except that the *dotted line* and *curve* illustrate another pair of  $\Delta$  and  $\delta$  obtained from fitting a different portion of the data. In this fit  $\delta$  is approximately zero, but  $\Delta$  is non-zero

also distinguishes the very stiff material from the others. Hence, the bounds are adjusted based on this value of the slope.

- Empirically, the following scheme to adjust the bounds greatly speeds the subsequent fitting and slightly improves the accuracy of the algorithm. For values of the slope of the secant between 0.01 and 0.1, 0.1 to 0.5 and  $>0.5$ , the lower bound is moved in the cantilever advancing direction to truncate the amount of data within the bounds to 15, 10 and 5%, respectively. By removing data where contact has likely not yet occurred, this truncation simply eliminates the number of putative contact points that need to be examined. If the slope of the secant is  $<0.01$ , i.e. a very soft material, however, rather than truncating the dataset, the upper bound and lower bounds are both moved 5% opposite the cantilever advancing direction so as to retain 25% of the data.
- Once the bounds are adjusted, each datum in the subset is tested as a putative contact point by using a pair of best-fit curves as follows. A line is fit to the data beginning at the lower bound and ending one point prior to the candidate contact point. A quadratic or linear fit is made to the data starting at the candidate point and ending somewhere above the upper bound. How many points above the upper bound to include is also determined by the value of the slope of the secant. If the slope is greater than 0.5 (a very stiff material) we use a linear approximation and fit 75% of the data beyond the putative contact point. If the slope of the secant is between 0.01 and 0.5 we fit 30% of the post-contact data with a quadratic function. If the slope of the secant is less than 0.01 we use 75% of the post-contact data for the quadratic fit. This is because the maximum deflection of very soft materials is very small and using 75% rather than only 30% of the data helps ensure that we

incorporate some deflections greater than the noise level. These empirical guidelines have been found to provide sufficient data for robust estimates of the contact point while still keeping computational time reasonable.

- For each pair of best-fit curves three measures are calculated: (1) the RMS value to provide an estimate of the goodness of fit; (2) the discontinuity between the end of the linear fit and the beginning of the quadratic fit ( $\delta$  in Fig. 5b, c); (3) the difference between the end of the linear fit and the nadir of the quadratic fit ( $\Delta$  in Fig. 5b, c, Table 1).
- RMS,  $\delta$  and  $\Delta$  for all of the regression pairs are then scaled so that each measure has a mean value between 1 and 10. The scaling is done to help ensure that the sum is not overly weighted by extreme values of one of the measures. The three scaled measures are added and the first post-contact point in the pair of regressions with the lowest sum is designated to be the contact point.

The algorithm for this scheme is implemented in Matlab. Additionally, once the contact point is determined, each deflection curve is plotted, with the contact point clearly identified, to allow visual assessment (as shown in Fig. 5a).

All of the above guidelines for implementing the algorithm were based on materials with linear stress–strain laws.

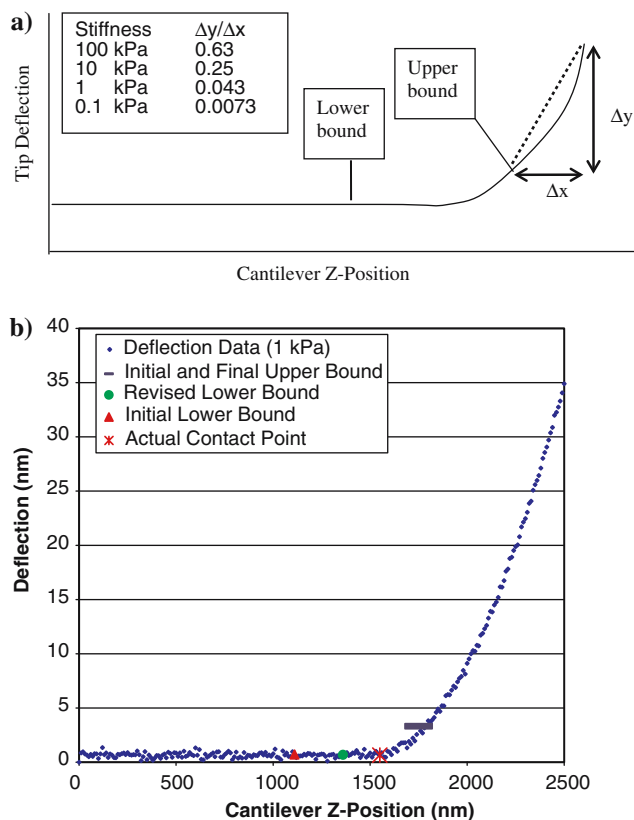


**Fig. 6** a. Illustration of how an initial estimate of material stiffness is estimated by the slope of the secant. This estimated stiffness is only used to adjust the bounds of the data within which the contact point is likely to be found. b. The results of adjusting the bounds based on the slope of the secant value obtained as described in Fig. 6a is illustrated for a 1 kPa material. The contact point is shown by the asterisk

Since, in practice, one does not know a priori the type of material being examined, it is important to see how well the algorithm identifies the contact point for nonlinear materials. Therefore, we applied the same guidelines and approach to identify the contact point for the simulated deflections curves for the three types of nonlinear materials.

Another method for identifying the contact point using a two-parameter Monte Carlo optimization to fit a section of the post-contact portion of the deflection curve with the free parameters being the contact point and the elastic modulus was proposed (Rotsch et al. 1999). This method identified the contact point and the elastic modulus simultaneously. It should be noted that this method assumes that the tip is an ideal cone and that the material has a constant elastic modulus. For all the simulated data for linear and nonlinear materials, the contact points identified by this method were compared to ours.

### 2.3 Mechanical properties

Once the contact point is identified, the deflection curve is converted back to a force-indentation curve from which we determined the mechanical properties of the material as previously described (Costa and Yin 1999). Specifically, we computed an apparent point-by-point elastic modulus ( $E_{pp}$ ) as a function of indentation depth using Eqns. 1, 2 and 3. To further ascertain how well the algorithm works for the three types of nonlinear materials, we generated indentation force–depth curves, based on the contact point identified by the algorithm, and compared the indentation depth dependence of  $E_{pp}$  obtained from those curves with the previously obtained finite element simulation force–depth relationship. If the contact point was identified correctly, the same relationships should be obtained.

### 2.4 Effects of misidentifying the contact point

To assess the effect of misidentifying the contact point on the simulated  $E_{pp}$  – indentation depth relationship, we purposely misidentified the contact point of the simulated deflection curves for the linear material with a modulus value of 10 kPa and for the MR, polynomial, and exponential materials. We examined the effects of missing the contact point by up to

**Table 1** Summary of the suggested search parameters for identifying the contact point for linear materials of various stiffnesses

Slope of the secant value (stiffness characterization)	Amount of deflection data in revised bounds(%)	Post-contact fit type	Post-contact data fit (%)
0.5–1.0 (Very stiff)	5	Linear	75
0.1–0.5 (Moderately Stiff)	10	Quadratic	30
0.01–0.1 (Moderately Soft)	15	Quadratic	30
< 0.01 (Very Soft)	25	Quadratic	75

**Table 2** Results of our approach to identifying the contact point with and without simulated noise equivalent to 0.25 nm of deflection

	Modulus of linear material (kPa)					Material type		
	0.1	1	10	50	100	MR	POLY	EXP
No noise	0	0	0	0	0	+3	+2	> -25
Noise	+2	-1	-1	-1	-1	-2	+1	> -25
Rotsch algorithm	> -25	+4	+4	0	+4	0	-10	> +25
Calculated $E_{pp}$ (kPa)	0.094	1.02	10.22	51.67	103.83	NA	NA	NA

The results for the same noisy data using the algorithm proposed by Rotsch et al. are also shown. The number listed is the number of data points by which the contact point was misidentified. The sign (+/-), indicates the direction (prior/after) in which the contact point was missed. One data point for the linear materials equals 10 nm and for nonlinear materials equals approximately 5 nm. The asymptotic values of the elastic modulus obtained from the force-depth relationships, based on the identified contact point, for the linear materials are also shown

ten data points (100 nm), before and after the actual contact point for the linear material and up to five data points for the nonlinear materials. For each of these misidentified indentation force-depth curves, we calculated the depth dependence of  $E_{pp}$  as described above.

### 2.5 Effects of noisy data

To realistically account for the effects of noise in the simulations, we first determined the standard deviation of the noise in the region spanning 400 nm of piezo travel in the pre-contact region of several typical deflection curves obtained from cells. The standard deviation of the noise averaged approximately 0.25 nm. Thus, noise with standard deviations of 0.15, 0.25 and 0.35 nm was randomly added to the raw simulated data using the *randn* function to attain simulated, “noisy” deflection curves. The resulting “noisy” force-depth curves were then analyzed as above.

Finally, to assess the combined effects of both noise and misidentifying the contact point, we generated force-depth curves with the contact point misidentified over the same range as above for the linear material but with random noise with a standard deviation of 0.25 nm added.

## 3 Results

### 3.1 Identifying the contact point

The accuracy of identification of the contact points predicted by our algorithm, as well as the alternative one by Rotsch et al, for all of the simulated deflection curves are summarized in Table 2. Even though our algorithm was developed for linear materials, it is able to correctly identify the contact point within three data points for the nonlinear MR and POLY materials. Additionally, even in the presence of noise, for all the linear materials and for all but the material with an exponential stress-strain law, the predicted contact point is within two points of its actual value. For the softest material, the algorithm performs remarkably well considering that the maximum deflection of that curve is only approximately ten times the noise level. The asymptotic values of  $E_{pp}$  obtained

from the force-depth relationships for the linear materials, based on the automatically identified contact point in the presence of noise, are also shown in Table 2. It is clear that the contact point is identified sufficiently closely to obtain values of the elastic modulus that, at worst, are within about 3% of the correct value.

The algorithm proposed by Rotsch et al. performed more poorly than ours for all but the MR material. The fact that it performs very poorly for the softest material suggests that it is also more sensitive to the signal-to-noise ratio than our algorithm. Also, one can see that the algorithm performs much more poorly as materials get more non-linear. This is not at all unexpected since that algorithm assumes that the material being indented has a constant elastic modulus.

### 3.2 Effects of misidentifying the contact point

The effects of misidentifying the contact point, assessed in terms of the  $E_{pp}$  – indentation depth curves, are shown in the panels of Fig. 7. The results for a linear material are shown in Fig. 7a. The  $E_{pp}$  values for the initial 200 nm of indentation may be incorrect by more than an order of magnitude if the contact point is missed by five points (50 nm) or more but they asymptotically approach the correct value at sufficiently high indentation depths. The amount of indentation necessary to approach the correct value increases the more the contact point is missed. Figure 7b illustrates the effect of misidentifying the contact point for a MR material. As with the linear material there is a similar asymptotic approach to the correct value with increasing indentation – even though  $E_{pp}$  is no longer constant with indentation depth. Figures 7c, d illustrates the effects for the POLY and EXP materials, respectively. For both types of materials an error in identifying the contact point does not change the overall depth-dependence of  $E_{pp}$  but, like the linear materials, the greater the misestimation of contact point, the larger is the range of uncertainty for  $E_{pp}$  at any depth. For the POLY material, as indentation depth increases the error bounds decrease such that at depths greater than 200 nm the estimated values of  $E_{pp}$  are well within a factor of two of being correct. For the EXP material, however, a different trend is observed. For indentation depths of about 100 up to 200 nm the estimates



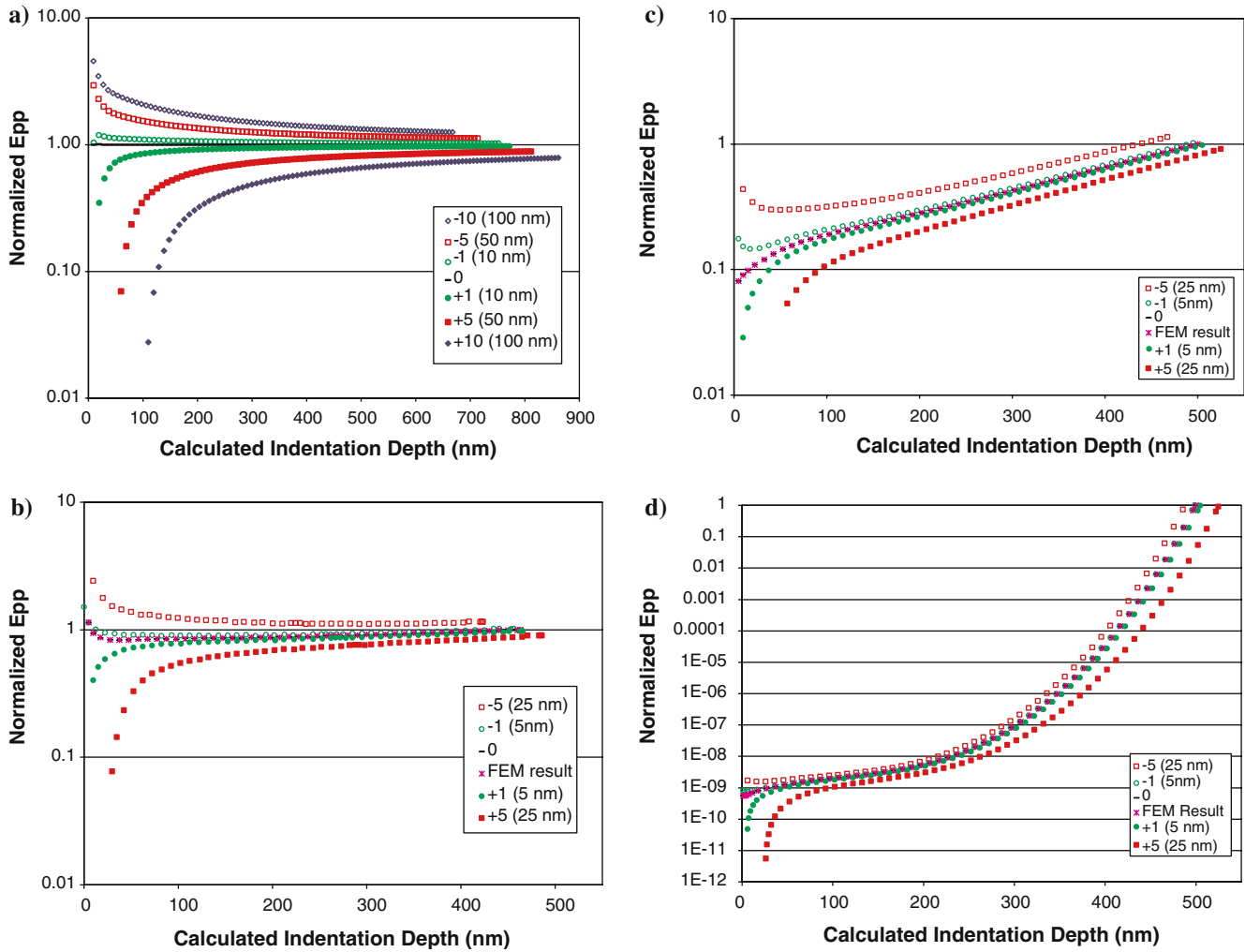


**Fig. 7** Semi-logarithmic plots of apparent, point-by-point elastic modulus as a function of indentation depth showing the effect of misidentifying the contact point for **a** a linear material with an elastic modulus of 10 kPa; **b** a material with nearly linear (Mooney–Rivlin) stress–strain law – results obtained from the finite-element model (FEM) are also shown.; **c** a material with a polynomial stress–strain law; **d** a material with an exponential stress–strain law. The data are normalized so that the  $E_{pp}$  of the correctly identified contact point is 1. The + and – signs associated with each symbol indicate misidentification prior to or after the actual contact point

of  $E_{pp}$  are within a factor of 2 but rather than decreasing as indentation increases, the error bounds increase to an order of magnitude or more beyond 400 nm. Note, that the effects on the error bounds for both linear and nonlinear materials are not symmetric – identifying contact incorrectly “before” results in greater error than “after” the true contact point.

### 3.3 Effects of noisy data

The effects of varying levels of noise on the resulting  $E_{pp}$  – indentation depth curves for linear materials are shown in Fig. 8. As with misidentifying the contact point, the effects of noise are most severe at indentations less than about 100 nm. The predictions asymptotically approach the true value at larger indentation depths. Unlike missing the contact point, however, higher noise levels do not cause further devi-

ations of the asymptotic value from the actual value. In fact, for larger indentations, the results seem to be independent of the noise level.

The combined results of noise and misidentifying the contact point by differing amounts are shown in Fig. 9a. Compared with Fig. 7a, it appears that there is not a large additional effect of noise on the estimation of  $E_{pp}$ . This is explicitly demonstrated in Fig. 9b which is a plot of the differences in  $E_{pp}$  between Figs. 7a and 9a. The limited influence of noise confirms the impressions of Fig. 8.

## 4 Discussion

Our results demonstrate the ability of the algorithm to accurately identify the contact point, even in the presence of noise of the level typically observed in AFM studies. Additionally,

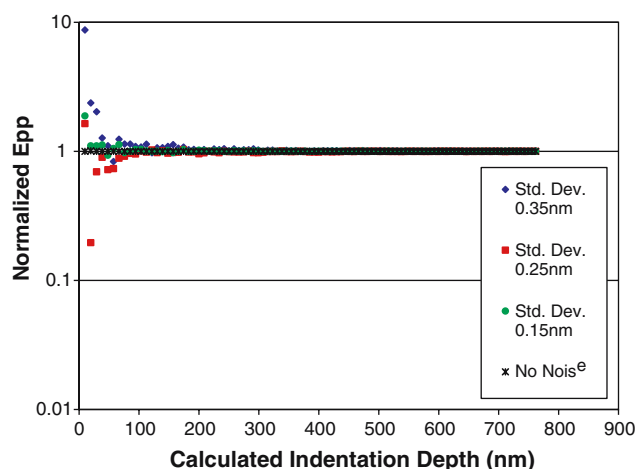


**Fig. 8** Similar to Fig. 7 except illustrating the effect of random noise on the apparent, point-by-point elastic modulus of a linear material. For comparison, the results with no noise are also shown. Sample deflection curves on cells have a noise level with a standard deviation of approximately 0.25 nm

even though the algorithm was developed based on behavior of linear materials, the contact point can be identified accurately for certain nonlinear materials, namely MR and POLY material types. However, as shown in Table 2, the contact point for materials with exponential stress–strain laws of the type we examined could not be identified reliably – likely due to the extremely wide range of stiffnesses of this type of material. This, in addition to the fact that the error bounds for the apparent modulus increase as indentation depth increases, are potential limitations one needs to keep in mind when determining mechanical properties for materials with this type of stress–strain law. These results highlight the importance of knowing the type of material that is being examined but this is not usually known a priori. Fortunately this conundrum can be easily resolved because, as previously reported, the depth dependence of the apparent modulus is distinctly different among the linear and nonlinear material types (Costa and Yin 1999). This is because materials with nonlinear properties had subtle, but clearly evident, deviations from the quadratic force–depth relationship characterizing a linear material. Properly accounting for tip geometry and calculating an apparent, point-by-point elastic modulus not only enable quantification of mechanical properties without the limitations of the Hertzian contact method (discussed in more detail below), but also does not require a priori knowledge or assumptions about the type of material. This is because the point-by-point method is the ultimate piecewise linear approximation to a nonlinear function.

One important additional finding of the current study is that the basic shapes of the  $E_{pp}$ –depth relationships are preserved for all types of materials, regardless of whether the contact point is accurately determined – at least within the range of values we examined. For linear, MR and POLY materials misidentifying the contact point results in an uncertainty for  $E_{pp}$  that is bounded. The uncertainty depends upon both the material type and the amount of misidentification of the

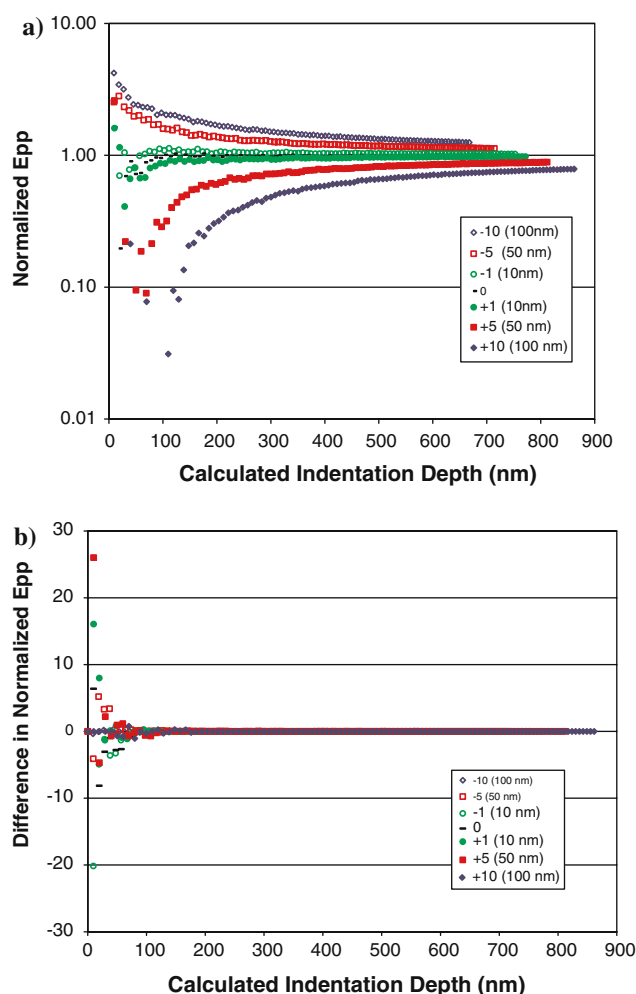


**Fig. 9 a** Similar to Figs. 7 and 8 except illustrating the combined effects of misidentifying the contact point (10 points prior to and after the actual contact) and noise (0.25 nm) on the elastic modulus of a linear material. **b** Pointwise differences between the normalized elastic modulus curves shown in Fig. 9a and those shown in Fig. 7 to highlight the effects of noise

contact point. Therefore, if one is not confident that the algorithm has accurately identified a contact point and the resulting estimations of apparent modulus, one can employ the following alternative procedure. Select a group of potential contact points thereby resulting in a range of possible values of the apparent modulus. This estimation might suffice for some applications. Alternatively, if one can identify contact points that are clearly before and after the unknown actual contact point, one will obtain an upper and lower bound for the apparent modulus. Progressively moving these putative contact points closer together should enable more precise estimations of the apparent modulus.

Our approach was developed for linear materials with a certain range of stiffnesses and a specific value for the cantilever stiffness. This does not mean that data for softer or harder materials or other cantilever stiffnesses cannot be analyzed. Rather the results should be viewed as guidelines suitable for relative cantilever to material stiffnesses in the range we

examined. Of course, in practice one does not know a priori how stiff the material is. Thus, it is clear that some empiricism and insight need to be utilized to obtain accurate results. Nevertheless, since the algorithm performed well over several orders of magnitude of material stiffnesses, we expect it to be widely applicable.

A general guideline for choosing a cantilever stiffness to match the material being indented would be to select a cantilever that yields, on average, deflection curves that appear much like the 1–10 kPa curves presented here. Specifically, the cantilever is sufficiently soft, relative to the material being indented, to provide substantial deflection relative to the noise level of the signal, but stiff enough to still allow substantial indentation. Moreover, there must be sufficient pre-contact data to allow estimation of the noise level, there must be sufficient deflection to allow accurate fitting of data beyond the upper bound, and there should not be large pre-contact anomalies such as jumps or “snap-to” effects. It should be pointed out that the approach described herein for the algorithm, i.e. the amount of data to include to estimate noise, the initial estimate of the material stiffness and the bounds and amount of data to use for the fitting, etc. are simply guidelines based on our experience and are validated by our simulations. In other situations, slightly different guidelines might pertain. Clearly some judgment is still required to analyze complicated AFM data, but the approach outlined herein should both facilitate data analysis and also provide considerably more confidence in the interpretations than the approaches currently being used. As long as one is cognizant of these constraints when the AFM indentation data are being acquired, the proposed approach and the estimated material properties are likely to be reasonably close to the real values.

The results for linear materials indicate that the elastic modulus asymptotically approaches the correct value at sufficiently large indentation depths – even if one misidentifies the contact point by a few data points. Similar results for analysis of indentation of polymer gels were also recently reported (Dimitriadis et al. 2002). While the asymptote provides the most accurate assessment of the stiffness of linear materials, one must recognize that the equations on which the point-by-point modulus is based, assume an infinite half-space. This implicitly presumes that there is no effect of the substrate – no matter how large the indentation. Clearly this is not the case. Depending upon the thickness of the material, once a certain amount of indentation is exceeded, the mechanical properties of the substrate will affect the data. We previously reported an analysis of this effect for flat indenters and suggested guidelines to minimize substrate effects (Karduna et al. 1997). Similar analyses for more complex tip geometries have also been reported (Costa and Yin 1999; Jaffar 1995). These studies provide a basis for deciding in other situations whether this important assumption is reasonable.

There are several other aspects of the approach that deserve further discussion. First, the tip geometry-dependent equations presented earlier are used only to obtain the simulated deflection curves for the various materials. Identification of the contact point does not require any implicit

assumptions about the shape of the cantilever tip. Second, while the value of 0.5 used for Poisson’s ratio is not correct for nonlinear materials, the point-by-point modulus is effectively a pointwise linear approximation for nonlinear materials. Therefore, using that value is defensible and, moreover, will not affect any of the interpretations with respect to the influence of contact point identification on the estimated  $E_{pp}$  since the same factor is used regardless of the contact point. Third, it is important to emphasize that the initial, crude estimate of stiffness based on the slope of the secant is only used to restrict the number of possible contact points to test and to inform the amount of data to include in the fitting portion of the algorithm to identify the contact point. Once the contact point is identified, the subsequent analysis to estimate material properties is not affected or limited by the amount of data used in the fitting. Using these restrictions to search for the contact point may be why the algorithm performs fairly well, even for materials with nonlinear stress–strain laws. In contrast, the algorithm proposed by Rotsch et al. cannot be used to analyze nonlinear materials because their approach explicitly assumes a linear material. Finally, not only does the present algorithm appear to accurately identify the contact point, but restricting the search range also reduces considerably the computational time. For example, a complete analysis of 64 indentations, each containing 256 data points, was completed in less than 20 s on a Dell OptiPlex GX260 with a 2.4 GHz Pentium 4 processor and 256 MB of RAM. This is many times faster than multi-parameter optimizations, especially of the Monte-Carlo type. This can be important when many curves are being analyzed, such as in force mapping. Although the proposed method is automatic, it is still desirable to visually inspect the data to ascertain that the estimated contact point is reasonable. Based on the quality of the data, the type of material being examined, and the experimental conditions, i.e. indenting in air or under fluid, one can then decide whether this automatic approach is justified.

The most common approach to assessing mechanical properties from AFM indentation data is to fit the entire tip deflection (force) – indentation depth relationship to a quadratic function from which a Young’s modulus is estimated based on Hertzian contact mechanics. This contact mechanics approach implicitly assumes three things: (1) the tip is a smooth curved surface; (2) the deformations under the tip are infinitesimally small; and (3) the material has a linear stress–strain law and, as shown herein, is relatively soft. As our results indicate, in general indentations greater than about 100 nm are necessary to distinguish signal from noise and indentations greater than 200 nm may be needed to accurately estimate material properties – depending on how much one misidentifies the contact point. This need for indentations of this amount must be viewed in the context that most AFM cantilever tips are spherical caps of approximately 30 nm in diameter merging into a pyramid. Indentations sufficiently large to allow one to confidently estimate material properties clearly violate the assumption of infinitesimally small deformations under the tip that are needed for contact mechanics to pertain. Moreover, since the force – depth relationship

beyond the initial spherical cap region is dominated by the pyramidal geometry of the tip, assuming a spherical geometry for all indentation depths is also not valid. All of these considerations render using analyses based on Hertzian contact mechanics problematic. This issue has been addressed in more detail in recent publications (Costa and Yin 1999; Costa, et al. 2006).

## References

- A-Hassan E, Heinz WF, Antonik MD, D'Costa NP, Nageswaran S, Schoenenberger CA, Hoh JH (1998) Relative microelastic mapping of living cells by atomic force microscopy. *Biophys J* 74:1564–1578
- Bowen WR, Lovitt RW, Wright CJ (2000) Application of atomic force microscopy to the study of micromechanical properties of biological materials. *Biotechnol Letts* 22:893–903
- Briscoe BJ, Sebastian KS, Adams KS (1994) The effect of indenter geometry on the elastic response to indentation. *J Phys D: Appl Phys* 27:1156–1162
- Burnham NA, Colton RJ (1989) Measuring the nanomechanical properties and surface forces of materials using an atomic force microscope. *J Vac Sci Technol* 7:2906–2913
- Cleveland JP, Manne S, Bocek D, Hansma PK (1993) A nondestructive method for determining the spring constant of cantilevers for scanning force microscopy. *Rev Sci Instrum* 64:403–405
- Costa K, Yin FCP (1999) Analysis of indentation: implication for measuring mechanical properties with atomic force microscopy. *Trans ASME J Biomech Eng* 121:462–471
- Costa KD, Sim AJ, Yin FCP (2006) Non-Hertzian approach to analyzing mechanical properties of endothelial cells probed by atomic force microscopy. *ASME J Biomech Eng* 128: 176–184
- Cumpson PJ, Hedley J, Zhdan P (2003) Accurate force measurement in the atomic force microscope: a microfabricated array of reference springs for easy cantilever calibration. *Nanotechnology* 14:918–924
- D'Costa NP, Hoh JH (2005) Calibration of optical lever sensitivity for atomic force microscopy. *Rev Sci Instrum* 66:5096–5097
- Dimitriadis EK, Horkay F, Maresca J, Kachar B, Chadwick RS (2002) Determination of elastic moduli of thin layers of soft material using the atomic force microscope. *Biophys J* 82:2798–2810
- Gibson CT, Weeks BL, Abell C, Rayment T, Myrha S (2003) Calibration of AFM cantilever spring constants. *Ultramicroscopy* 97:113–118
- Heinz WF, Hoh JH (1998) Measuring the nanomechanical properties and surface forces of materials using an atomic force microscope. *Biophys J* 76:528–538
- Heinz WF, Hoh JH (1999) Spatially resolved force spectroscopy of biological surfaces using the atomic force microscope. *Nanotechnology* 17:143–150
- Hofmann UG, Rotsch C, Parak WJ, Radmacher M (1997) Investigating the cytoskeleton of chicken cardiocytes with the atomic force microscope. *J Struc Biol* 119:84–91
- Hutter JL, Bechhoefer J (1993) Calibration of atomic-force microscope tips. *Rev Sci Instrum* 64:1868–1873
- Jaffar MJ (1995) Stresses and deformations in elastic layers indented by a conical punch. *J Mech Eng Sci* 209: 201–205
- Jensen F (1993) Z calibration of the atomic force microscope by means of a pyramidal tip. *Rev Sci Instrum* 64:2595–2597
- Karduna AR, Halperin HR, Yin FCP (1997) Experimental and numerical analyses of indentation in finite-sized isotropic and anisotropic rubber-like materials. *Ann Biomed Eng* 25:1009–1016
- Lal R, John SA (1994) Biological applications of atomic force microscopy. *Am J Physiol* 266:C1–C21
- Mathur AB, Collinsworth AM, Reichert WM, Kraus WE, Truskey GA (2001) Endothelial, cardiac muscle and skeletal muscle exhibit different viscous and elastic properties as determined by atomic force microscopy. *J Biomech* 34:1545–1553
- Radmacher M (1997) Measuring the elastic properties of biological samples with the AFM. *IEEE Eng Med Biol* 16:47–57
- Rotsch C, Jacobson K, Radmacher M (1999) The dynamics of active and stable edges in motile fibroblasts investigated by atomic force microscopy. *Proc Natl Acad Sci USA* 96:921–926
- Sader JE, Larson I, Mulvaney P, White LR (1995) Method for the calibration of atomic force microscope cantilevers. *Rev Sci Instrum* 66:3789–3798
- Sato M, Nagayama K, Kataoka N, Sasaki M, Hane K (2000) Local mechanical properties measured by atomic force microscopy for cultured bovine endothelial cells exposed to shear stress. *J Biomech* 33:127–135
- Scholl D, Everson MP, Jaklevic RC (1994) *In situ* force calibration of high force constant atomic force microscope cantilevers. *Rev Sci Instrum* 65:2255–2257
- Shroff SG, Saner DR, Lal R (1995) Dynamic micromechanical properties of cultured rat atrial myocytes measured by atomic force microscopy. *Am J Physiol* 269:C286–C292
- Smith ST, Howard LP (1994) A precision, low-force balance and its application to atomic force microscope probe calibration. *Rev Sci Instrum* 65:903–909
- Tao NJ, Lindsay SM, Lees S (1992) Measuring the microelastic properties of biological material. *Biophys J* 63:1165–1169
- Wu HW, Kuhn T, Moy VT (1998) Mechanical properties of L929 cells measured by atomic force microscopy: Effects of anticytoskeletal drugs and membrane crosslinking. *Scanning* 20:389–397